

We are IntechOpen, the world's leading publisher of Open Access books Built by scientists, for scientists

6,900

Open access books available

186,000

International authors and editors

200M

Downloads

Our authors are among the

154

Countries delivered to

TOP 1%

most cited scientists

12.2%

Contributors from top 500 universities



WEB OF SCIENCE™

Selection of our books indexed in the Book Citation Index
in Web of Science™ Core Collection (BKCI)

Interested in publishing with us?
Contact book.department@intechopen.com

Numbers displayed above are based on latest data collected.
For more information visit www.intechopen.com



Nanomaterial-Enhanced Receptor Technology for Silicon On-Chip Biosensing Application

Timothy Anton Okhai, Azeez O. Idris, Usisipho Feleni and Lukas W. Snyman

Abstract

Nanomaterials integration in biosensors designs are known to enhance sensing and signaling capabilities by exhibiting remarkably high surface area enhancement and intrinsic reactivity owing to their distinctive optical, chemical, electrical and catalytic properties. We present the synthesis and characterization of silver nanoparticles (AgNPs), and their immobilization on a silicon on-chip biosensor platform to enhance sensing capability for prostate specific antigen (PSA) - cancer biomarkers. Several techniques, including UV-Visible (UV-Vis) absorption spectrum, Fourier transforms infrared spectroscopy (FTIR), high resolution transmission electron microscopy (HRTEM), scanning electron microscopy (SEM) and field emission scanning electron microscopy (FESEM) were used for characterizing the AgNPs. The biochemical sensor consists of AgNPs immobilized on the receptor layer of a silicon avalanche mode light emitting device (Si AM LED) which enables on-chip optical detection biological analytes. A bio-interaction layer etched from the chip interacts with the evanescent field of a micro dimensioned waveguide. An array of detectors below the receptor cavity selectively monitor reflected light in the UV, visible, infrared and far infrared wavelength regions. AgNPs used as an immobilization layer in the receptor layer enhances selective absorption analytes, causing a change in detection signal as a function of propagation wavelength as light is dispersed. The analytes could range from gases to cancer biomarkers like prostate specific antigen.

Keywords: silicon avalanche mode LED, silver nanoparticles, biochemical sensors, optical sensor, nanomaterials, receptor technology

1. Introduction

Biosensors and lab-on-chip (LOC) devices have become a subject of growing professional interest world-wide. This is evident in the growing number of scientific publications, and the astronomical growth in the world market for biosensors and lab-on-chip devices over the past ten years. This has been possible, on a large part, due to rapid improvements in sensing techniques, innovation and growth in the development of new biomaterials such as conducting polymers, copolymers and sol-gels, multiplexing capabilities that promote versatility in new generation sensor devices, the possibility of integration on standard silicon integrated circuit chip,

and miniaturization possibilities down to micro- and nano-dimensions. Recently, researchers have been successful in developing light emitting devices that can be realized in standard silicon integrated circuitry, and have also proposed diverse applications for these in the future [1–5]. The main advantage of these devices may be the ease of integration into mainstream silicon manufacturing technology such as complementary metal oxide silicon (CMOS) and radio frequency (RF) bipolar technologies. Through recent research, light emission from silicon devices has been achieved in various reverse-biased p-n avalanche structures. This development has now been nomenclated as “silicon light-emitting diodes that operate in the reverse avalanche mode” (Si AMLEDs) [6–10]. If the detailed dispersion characteristics observed per solid angle for a particular device is known, it can enable the design of novel and futuristic on-chip electro-optic applications. Examples of such applications could include wavelength multiplexers for on-chip communication, diverse futuristic on-chip micro- and nano-dimensioned gas sensors and even on-chip biosensors [11–14]. In this chapter, a two-junction micro-dimension $p + -np +$ Silicon Avalanche-based Light Emitting Device (Av Si LED) has been analyzed in terms of radiation geometrical dispersion characteristics, and with particular interest in the different wavelengths of light (colors) being emitted at different emission angles from the surface of the device. It is worthy of note that the detailed dispersion characteristics will be a function of the device structure, the number of transparent over layers with each having different optical refractive index, and even the final topography or curvature of the various surface layers.

2. Light emitting characteristics from silicon AMLEDs

Light emitting devices (LEDs) have become a subject of growing research interest in recent times. A series of LEDs have been realized in standard Complementary Metal Oxide Silicon (CMOS) technology by Kramer et al., [15] and Snyman et al. in [15–19]. These structures emit light through phonon-assisted intra-band and inter-band recombination phenomena [20–22]. Subsequent devices were developed by Du Plessis et al., which showed increased light emission when additional carriers are injected into avalanching Si $n + p$ light emitting junctions [23, 24]. Further work by Xu et al. led to the realization of a series of CMOS integrated LED devices with third terminal gated control [8]. Subsequently, the temperature, carrier density, and electric field encountered in Silicon Avalanche Mode Light Emitting Devices (Si AMLEDs) were analyzed by Duttal and Steeneken et al. They also suggested operation of gated Si LED operating in the forward-biased mode and emitting in the 1100 nm region [12]. A major advantage with these devices is the realization of high modulation speeds ranging into the GHz due to the reverse bias configuration of Si AMLEDs [25, 26]. Potential applications of these devices can be found in hybrid optical RF systems, on-chip micro-photonic systems, and CMOS-based optical interconnect. In a recent work by Xu and Snyman, they demonstrated enhanced emission intensities of 0.1 to about 200 $nW/\mu m^2$ from Si AMLEDs in the 650–750 nm emission regime by using enhanced impurity scattering and extended E-field profiling in the device [27, 28].

We present in this chapter a specific $p + np +$ graded junction type Si AMLED device (**Figure 1(a)**) that was realized in a 0.35 micron Si bipolar process with a high frequency RF application capability. This process enabled an “elongated pillar” structure to be etched out on a broad silicon semi-insulating p-substrate. These structures could hence effectively confine the lateral carrier diffusion and

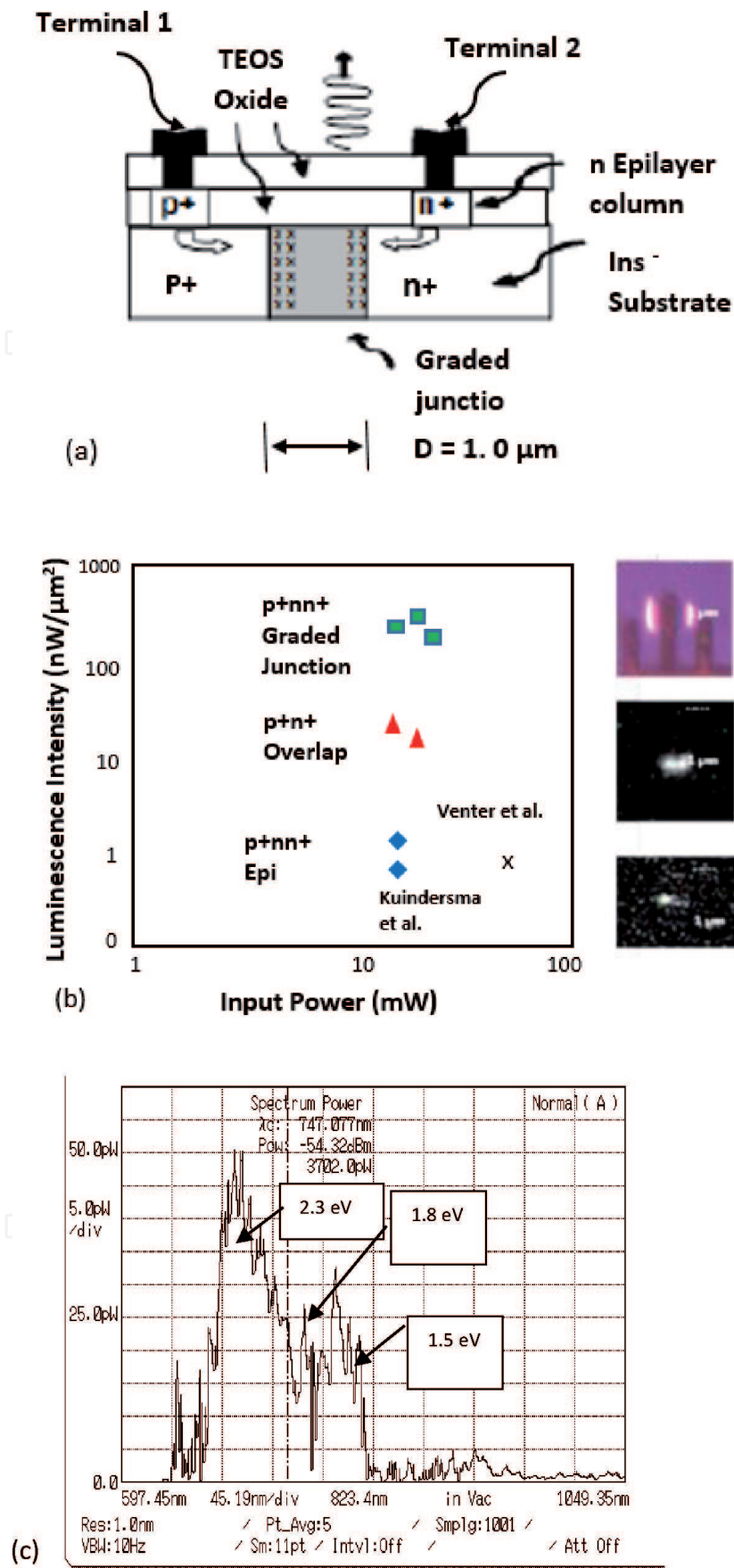


Figure 1. Device design (schematic), considerations of a $p + nn + \text{Si}$ avalanche mode LED in RF bipolar integrated circuitry [27] (a) lateral cross-section of the device. (b) Device optical performance characteristics as compared with other previous devices [27]. (c) Spectral characteristics of the emitted optical radiation (for below 570 nm consult Ref. [17]). Inserts show optical emission micrographs of the LEDs taken at normal angles to the surface of the device.

maximize the diffusing carrier density in the device. The device used n + and p + regions in the substrate region of the silicon, and positioned a distance 1 micron apart from each other. Subsequently, up to 1 micron graded doping profiles were formed at the edges of these regions, while overlapping of dopants occurred in the center region of the device [27]. For illustrative purposes, device design and performance characteristics relative to previous designs are again presented in **Figure 1(b)**. The optical emissions from the device were measured with an Anritso MS9710B Spectrum Analyzer with a lensed-probe optical fiber. The device and the lensed probe were electronically micro manipulated to within 0.1 mm of the light-emitting device. The total emission intensities with cross-sectional conduction areas of about 1 micron square as indicated at the surface of the device was measured to be in the order of 200 nW per μm^2 . **Figure 1(c)** depicts the main spectral components as observed for these types of devices. Clear peaks and prominent peaks of 2.8 eV, 2.3 eV, 1.8 eV, and 1.5 eV were observed in the spectrographic measurements for the devices and are shown in the spectrum when converting the nm emissions to corresponding eV emissions [19, 27]. Overall, the spectrum represent a broad spectrum from 450 nm to about 850 nm with main characteristic peaks at 450 nm (2.8 eV) (blueish), 550 nm (2.0 eV) (greenish), 600 nm (2.3 eV) (reddish), and at 750 to 850 nm (1.5 and 1.8 eV) (infrared). To form the on-chip biosensor, a bio-interaction layer etched from the Si AMLED chip interacts with the evanescent field of a micro dimensioned waveguide. An array of detectors below the receptor cavity selectively monitor reflected light in the UV, visible, infrared and far-infrared wavelength regions.

AgNPs used as immobilization layer in the receptor layer enhances sensitivity and selective absorption of antigens and biomarkers, like the prostate specific antigen (a biomarker for prostate cancer), causing a change in detection signal as a function of propagation wavelength as light is dispersed.

3. Transducers and transduction mechanisms in biosensors

Integrated biosensors can be categorized in several ways, one of which is their transduction mechanism. Below is a brief description of some of the main transducers used in biosensor mechanisms:

3.1 Transduction mechanisms

Electrochemical or Electroanalytical transducers: These types of transducers exploit analyte capturing to change the electrochemical characteristics of electrode-electrolyte systems. Hassibi, and Lee [29] described one of the first reports of a CMOS electrochemical biosensor array chip capable of performing impedance spectroscopy, amperometric analysis, and cyclic-voltammetry techniques. The Electrical performance of this CMOS multi-functional chip is comparable to state-of-the-art electrochemical measurement instruments currently used in molecular biology. Prior efforts in this area are limited only to ISFET [30] and conduction-based sensor arrays [31] in CMOS compatible processes.

Mechanical transducers: Mechanical transducers in biosensors are systems in which an electromechanical parameter of the system (e.g., mass of a cantilever) is changed by the additional mass of the captured analytes. Mechanical transducers cannot be fabricated using standard CMOS processes. This is largely because CMOS processes, unlike many MEMs processes, offer no component or device, which can move in response to mechanical motion [32, 33].

Thermal transducers: They are used to measure the temperature change during biological thermal reactions to detect the total number of molecules involved in the reaction [34].

Acoustic transducers: Acoustic transducers are based on the principle of using acoustic waves to develop biosensing devices. Acoustic waves can be used to analyze biochemical reactions in different fluid (liquid and gas) environments because they have the ability to travel through them easily. Different mechanisms can be employed to either generate or receive acoustic waves, including piezoelectric, magnetostrictive, optical and thermal techniques. The surface or the acoustic biosensor can be functionalized using standard methods, and the binding of the target analyte will induce a change in the acoustic wave. By measuring and subsequently analyzing this variation in the resonant frequency, it is possible to determine the correlation between the acoustic signal and the interaction of the molecule. One important advantage of acoustic transducers is the ability to operate using wireless excitation. This makes it extremely important for sensing in difficult-to-reach or hazardous environmental conditions. Additionally, the compatibility with integrated circuit technology permits a high efficiency in the fabrication process. The main drawback of this technique is the fact that any little vibration induced in the system can produce artifacts that will require complex algorithms to differentiate from the true biosensing signals [35].

Optical transducers: Optical biosensors can easily fulfill the requirement for high sensitivity, fast response and the potential for real-time measurements. They also lend themselves to optical measurements through different techniques like emission, absorption, fluorescence, refractometry, or polarimetry. Optical biosensors based on evanescent wave detection have unique properties such as extremely high sensitivity for direct, real-time measurement of biomolecular interactions in label-free schemes. The advantages of optical sensing are significantly improved when this approach is used within an integrated optics context. Integrated optics technology allows the integration of passive and active optical components (including fibers, emitters, detectors, waveguides, and related devices) onto the same substrate, allowing the flexible development of miniaturized compact sensing devices, with the additional possibility to fabricate multiple sensors on a single chip. The integration offers additional advantages such as miniaturization, robustness, reliability, potential for mass production with consequent reduction of production costs, low energy consumption, and simplicity in the alignment of the individual optical elements [36].

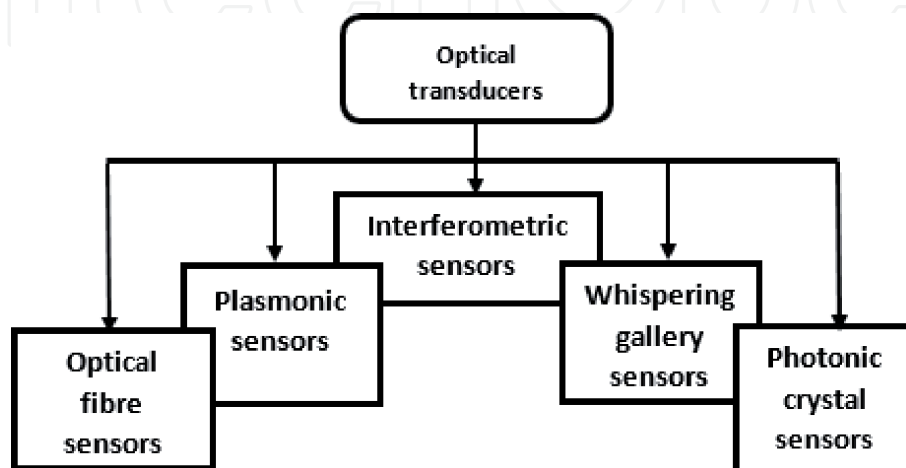


Figure 2.
Categories of optical transducers used for biosensor applications.

Independent of the transduction method used in integrated biosensors, one challenge is always to adequately immobilize capturing probes on the surface to create the capturing spot. Our design addresses this challenge by etching a receptor cavity through the silicon substrate, and by using AgNPs as immobilization layer in the receptor layer to enhance selective absorption of the target analyte.

3.2 Optical transducers categories

Optical transducers can be further categorized into the different categories shown in **Figure 2** above.

4. Waveguide structures

In waveguide structures, light is guided in the plane of the thin film, facilitating the integration of such a sensor, along with source and detector components, into a single integrated chip device [37]. This is a significant advantage in the development of on-chip micro- and nano-optical biosensors. Secondly, for porous silicon waveguides, the active sensing layer is the top porous layer, eliminating the infiltration difficulties that can plague Bragg mirrors, rugate filters, and micro-cavities, where biomolecules must filter through many layers of both high and low porosity. As a result of both advantages mentioned above, waveguide sensors display electric field confinement, sharp resonance peaks, and a thin sensing layer, all qualities that facilitate a fast response and a high sensitivity detection of molecules.

4.1 Optical waveguide biosensors

Various modalities have been developed for optical waveguide biosensor applications. They include grating-coupled waveguide sensors, interferometric waveguide sensors, photonic crystal waveguide sensors and resonant optical microcavity sensors, among others. **Figure 3** below provides examples for each of the optical waveguide options mentioned.

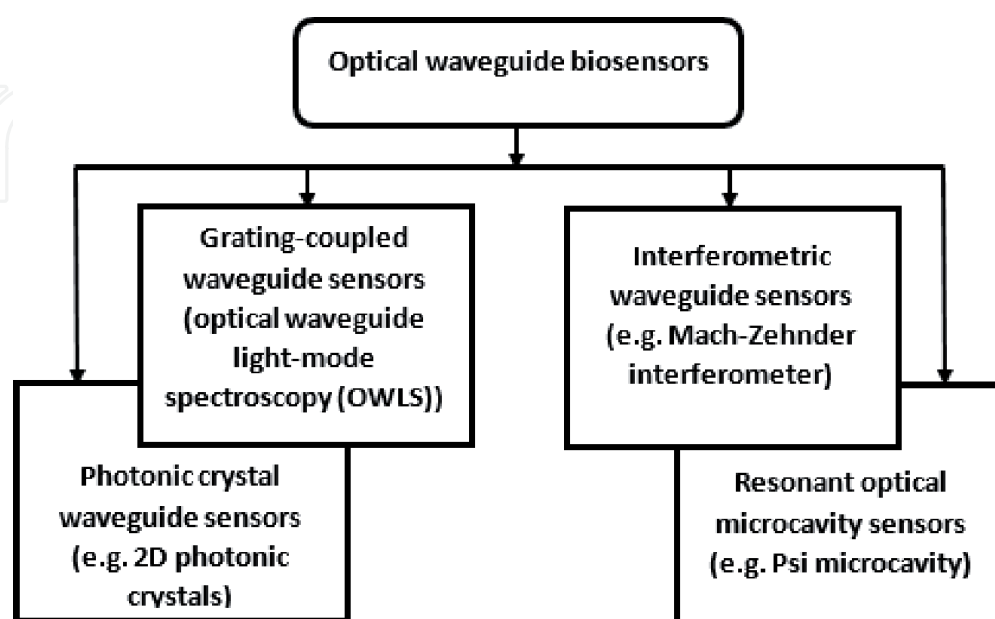


Figure 3.
Optical waveguide biosensor modalities and examples of their applications.

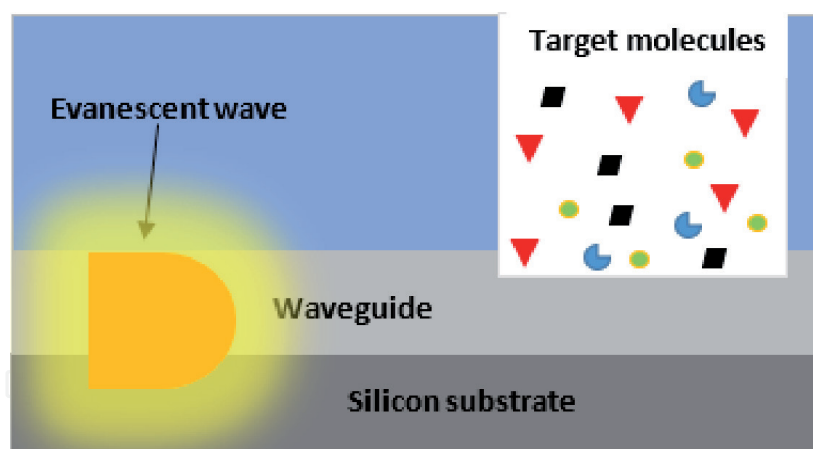


Figure 4. Schematic representation of an optical biosensor based on evanescent wave interaction. Due to interaction of the light with the target molecules (analytes) within the cavity in the interaction area, the optical wave undergoes a change in its propagation constant due to the variation in the effective refractive index.

4.2 Receptor layer in waveguide and evanescent field

The difference in refractive index between the core and cladding of an optical waveguide exist. Thus, light is guided via the core with a higher refractive index on account of total internal reflection, which generates an evanescent optical field that decays exponentially from the sensor surface, as in **Figure 4**. Biomolecular binding events modulate the refractive index contrast and thus attenuate the propagation of light through the waveguide. By monitoring the coupling and/or propagation properties of light through an appropriately modified waveguide, it is possible to construct sensors responsive to the target biomolecular analytes of interest, as shown in **Figure 4**.

5. Synthesis and characterization of nanomaterials

Silver nanoparticles were, characterized and applied in the receptor layer to enhance the sensitivity of the biosensor. The synthesis method and materials, and the characterization procedures and results are discussed in the following sections.

5.1 Synthesis procedure and materials

Silver nanoparticles were prepared by chemical reduction method, using silver nitrate (AgNO_3) as the silver precursor. The preparation procedure of silver nanoparticles is adopted from Muzamil et al., [38] with minor modification. All reagents were of analytical grade and used without any further purification. The reagents include Silver nitrate (AgNO_3 , $\geq 99\%$), Trisodium citrate ($\text{Na}_3\text{C}_6\text{H}_5\text{O}_7$, 1%), Polyethylene glycol ($\text{C}_2\text{nH}_4\text{n} + 2\text{O}_\text{n} + 1$, $\geq 99\%$), and Sodium hydroxide (NaOH , $\geq 99\%$), and were all purchased from Sigma Aldrich. The experiment was conducted at room temperature (23°C) unless otherwise stated. To synthesize silver nanoparticles, 50 ml of 1 mM silver nitrate solution and 5 ml of polyethylene glycol were taken and heated till boiling on a magnetic stirrer. When the solution started to boil, 1% trisodium citrate solution of 4 ml was quickly added with constant stirring. A few minutes later, the solution turned into yellow color, hinting the formation of silver nanoparticles. The pH of the nanoparticles was kept at 7.6 by adding NaOH. Afterward, it was cooled to room temperature and stored at 4°C before use.

5.2 Characterization of silver nanoparticles

The prepared AgNPs were characterized using SEM, FESEM, HRTEM, SAXS, FTIR Spectroscopy, and UV-Vis spectroscopy. The SEM images of samples were obtained from JEOL Scanning Microscope JSM-6400. The surface morphology and elemental analysis of the silver nanoparticles were studied using JSM-7800F Field Emission Electron Scanning Microscope (FESEM), integrated with energy-dispersive x-ray spectroscopy (EDS). High resolution TEM analysis was carried out using Hitachi H-800 electron microscope at 200 kV acceleration to determine the size distribution and elemental composition of samples respectively. Small angle x-ray scattering (SAXS) spectroscopy was performed with SAXSpace Spectrometer from Anton-Paar, Graz, Austria, using a solid sample. The X-ray scattering spectra were plotted with a SAXdrive software. GIFT software was used to Fourier transform the scattering data to obtain the pair distance distribution function (PDDF) and size distribution spectra. The functional groups of the nanomaterials were done on a Perkin Elmer FTIR spectrometer Frontier (Spectrum 100 spectrometer) in the range

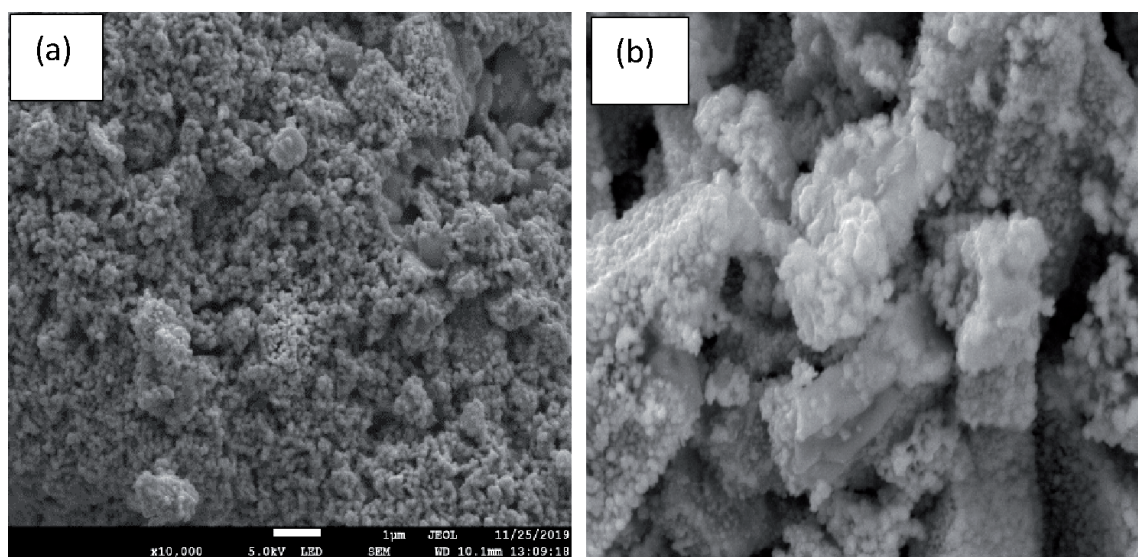


Figure 5.
Electro-micrograph image of (a) SEM analysis, and (b) FESEM analysis at a magnification of x10,000.

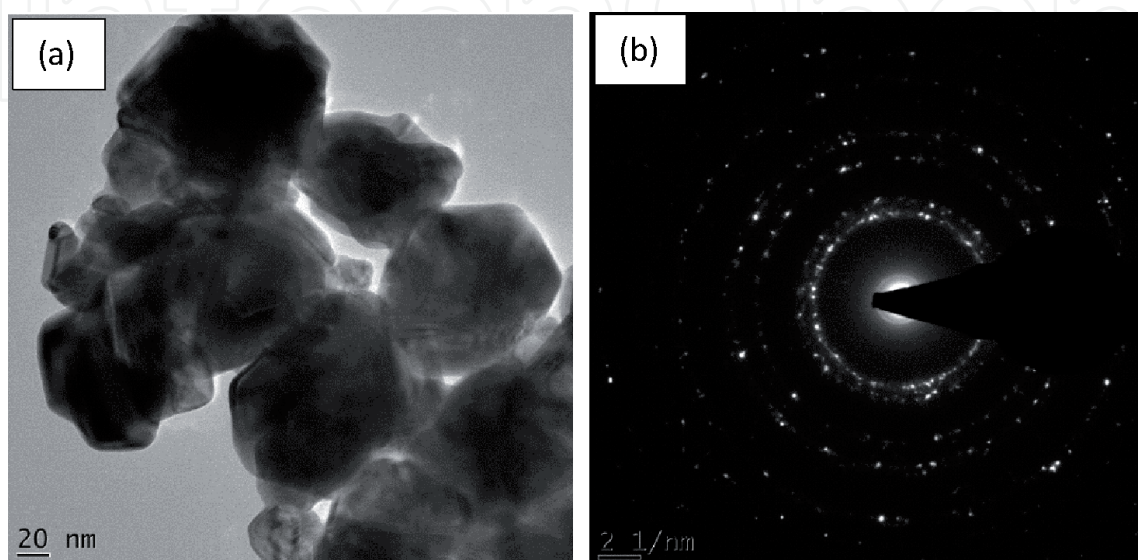


Figure 6.
(a) HRTEM electro-micrograph at 20 nm scale view and (b) SAED pattern of AgNPs.

of 400–4000 cm^{-1} using the KBr pellet method. UV-vis spectra were acquired over the range of 200–800 nm using PerkinElma Lambda 650S UV/Visible Spectrometer. To produce graphs and curves that are clear enough for reporting, Origin 8.0 software was used to plot the data obtained from the characterization equipment.

5.3 Results and discussion

Scanning electron microscope (SEM) and FESEM were used for topographical imaging of the nanoparticles, and to investigate the size, shape, impurities &

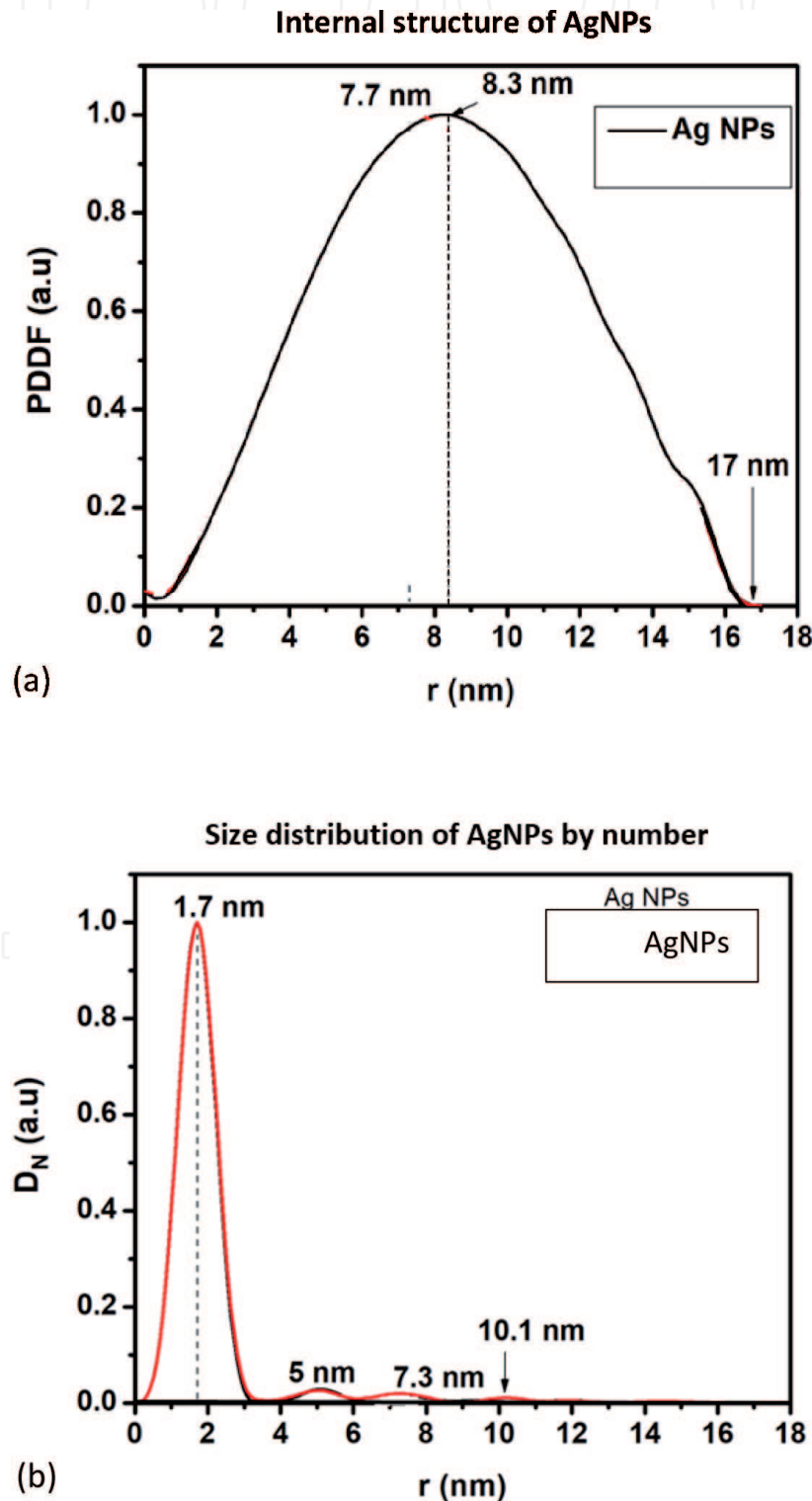


Figure 7.
(a) SAXS analysis showing (a) internal structure of AgNPs (b) size distribution by number.

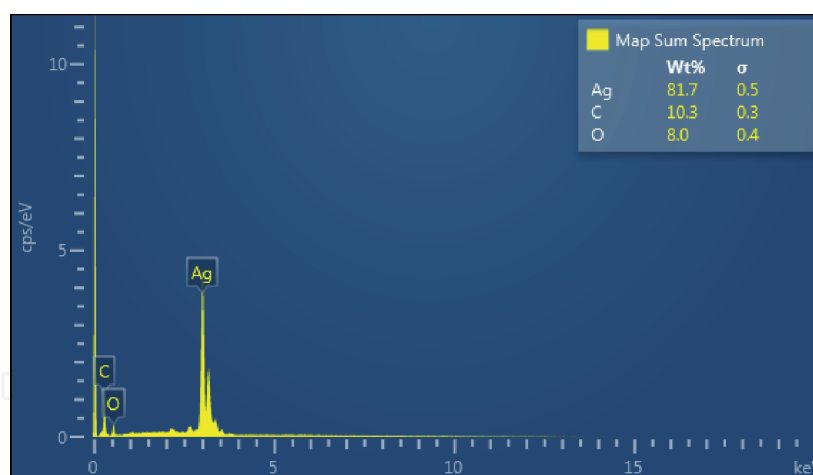


Figure 8.
EDS spectrum confirming the presence of silver, carbon and oxygen.

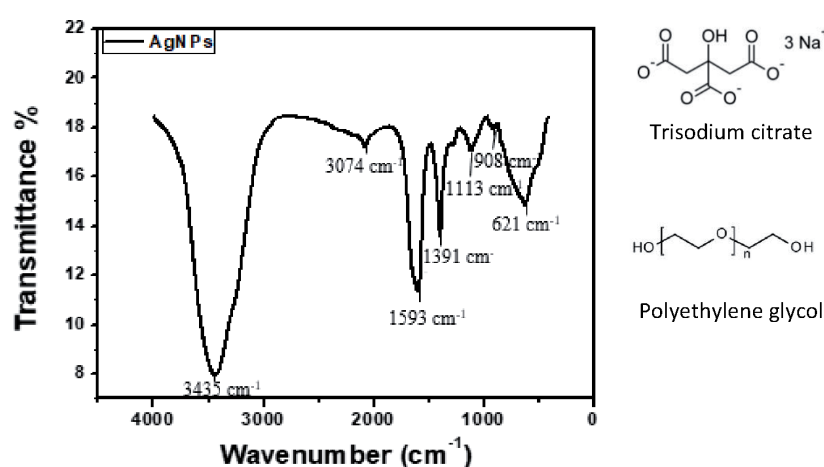


Figure 9.
FTIR graph showing prominent peaks representing the unique fingerprint of AgNPs that was synthesized.

stabilization of the particles, as shown in **Figure 5(a)** and **(b)**. The SEM image of the AgNPs shown in **Figure 5(a)** reveals a globular-shaped morphology, which was further confirmed by the FESEM image in **Figure 5(b)**. The FESEM confirmed the globular-cluster shaped morphology of the silver nanoparticles.

Interestingly, the HRTEM image in **Figure 6(a)** showed that the AgNPs are spherical at nano-range with spherically shaped internal structures. This is supported by the selected area diffraction structure (SAED) image in **Figure 6(b)**. HRTEM results also complement the SAXS results, which show that most of the particles are spherical or cuboidal in shape.

The SAXS analysis in **Figure 7** was used to investigate the internal structure of the nanoparticle, and it revealed that the AgNPs show lattice fringes, which confirms that the particles are crystalline. In addition, they exhibited a quasi-spherically shaped internal structure as expected. **Figure 7(a)** shows the internal structure of the AgNPs, while **Figure 7(b)** shows their size distribution by number.

The elemental composition of the AgNPs was evaluated by energy dispersion x-ray spectroscopy (EDS) to find out the purity of the nanomaterials. From the layered images and the EDS spectrum analysis, we confirm the presence of silver, carbon and oxygen, as shown in **Figure 8**. The presence of carbon was due to the carbon tape used for coating the nanomaterial before the analysis.

The morphology is consistent with the expectation for silver nanoparticles, and we functionalized our silver with polyethylene glycol. The sizes (width and

diameter) for the AgNPs could not be clearly determined due to agglomeration of the particles. In the FTIR analysis represented by the graph in **Figure 9**, prominent peaks were observed for different stretches of bonds. The peak at 3435 cm^{-1} , representing N-H stretch, 3074 cm^{-1} assigned to C-H stretching vibrations, and 1593 cm^{-1} corresponding to stretching vibration of C=O bond. The peak at 1391 cm^{-1} corresponds to C-C and C-N stretching, while 1113 cm^{-1} assigned to $\text{-C}=\text{C}$ bond, and 908 cm^{-1} and 621 cm^{-1} are for C-H out-of-plane bend and CH bending vibrations, respectively. These peaks are comparable to [39].

UV Visible spectroscopy is one of the most important techniques which can confirm that the prepared material are nanoparticles [40]. **Figure 10** shows the plot of absorption spectrum obtained from the UV-Vis spectroscopic analysis of the AgNPs over a range of 200 to 800 nm. The exact peaks occurred at 310 and 400, which is indicative of the peak of silver nanoparticles [41, 42]. The bandgap from the Tauc plot in **Figure 10(b)** for the synthesized AgNPs is 3.26 eV, which implies that the nanomaterials will absorb in the UV-Vis range.

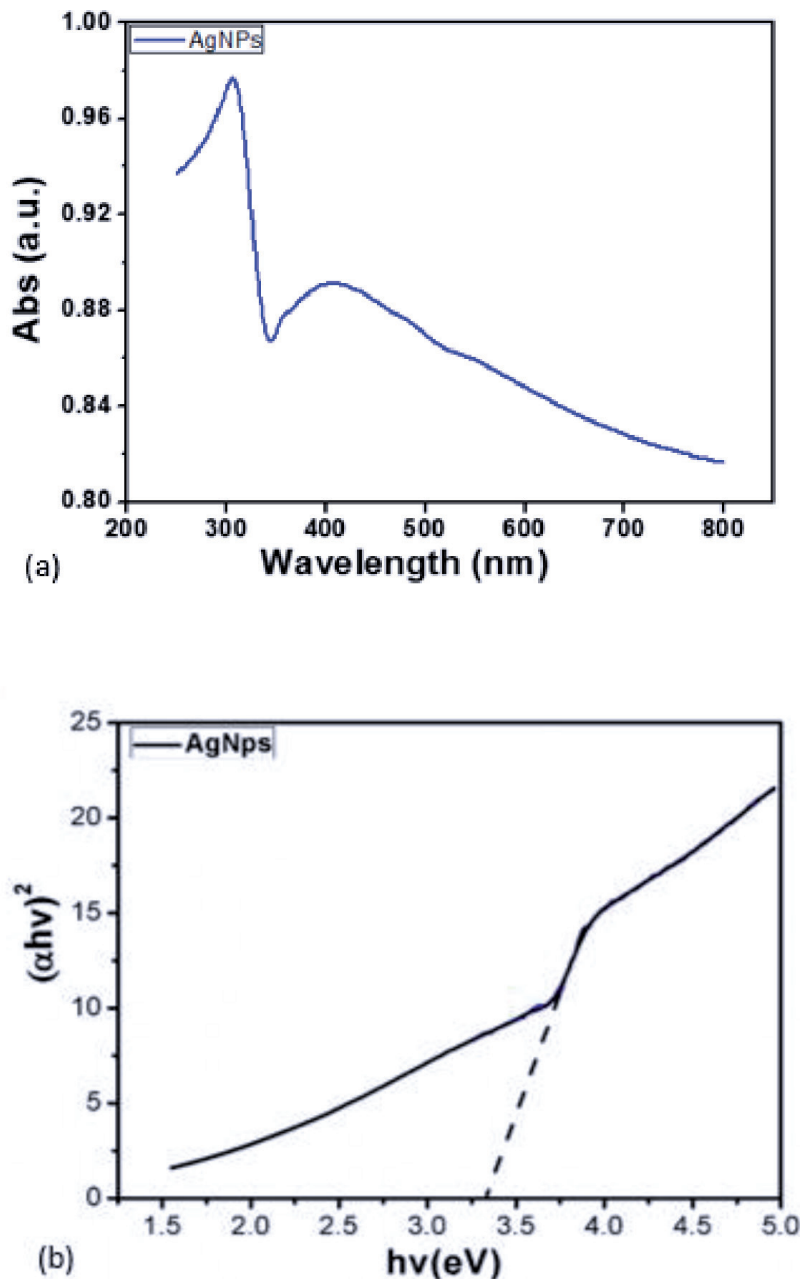


Figure 10. UV-Vis results for AgNPs showing (a) the absorption spectrum, and (b) the bandgap from Tauc plot.

6. Design, simulations and potential applications

We present in this section the design, simulation results and potential futuristic on-chip applications of our device.

6.1 Software simulation and design

To model how the evanescent waves would couple with bio-species in a cavity etched in the nitride layer as light waves travel through the waveguide, we performed optical simulations using RSoft BeamProp optical simulation software. As represented in **Figure 11**, light emitted from the optical source travels through the waveguide. As the resultant evanescent wave travels through the cavity etched deep into the nitride layer, it is exposed to specific analyte material trapped within the cavity. In this design, a multimode wave travels through high refractive index bridge waveguide and interacts with material within the etched cavity in the nitride layer. The interaction, in this case, would be primarily a function of the specific refractive index of the analyte inside that cavity, since the multimode light traveling in the waveguide will interact and be diverted into the absorbed analyte. The unique fingerprints of each material within the cavity then produces a change in signal that is recognizable by the detector, as in **Figure 11(a)**.

6.2 Applications in futuristic micro- and nano-dimensioned devices

Applications already proposed and demonstrated for Si Av LEDs include micro displays [44, 45] and Lab-on-chip systems [46, 47]. Analyses of test results from our device open up exciting possibilities for potential applications for the derived technology in futuristic integrated on-chip optoelectronic and biosensor applications.

These applications can be achieved through (1) placements of specific designed optical sources with specific directional and dispersive emission characteristics; (2) design and placement of micro wavelength dispersive coupling into micro dimensioned on-chip optical waveguides, and (3) design and placement of broadband wavelength emitters for diverse on-chip electro-optic applications. Other possible applications include (4) realization of various on-chip nano- and micro-dimensioned sensors that can detect a variety of parameters, ranging from standard physical parameters to a range of derived bio-parameters through the

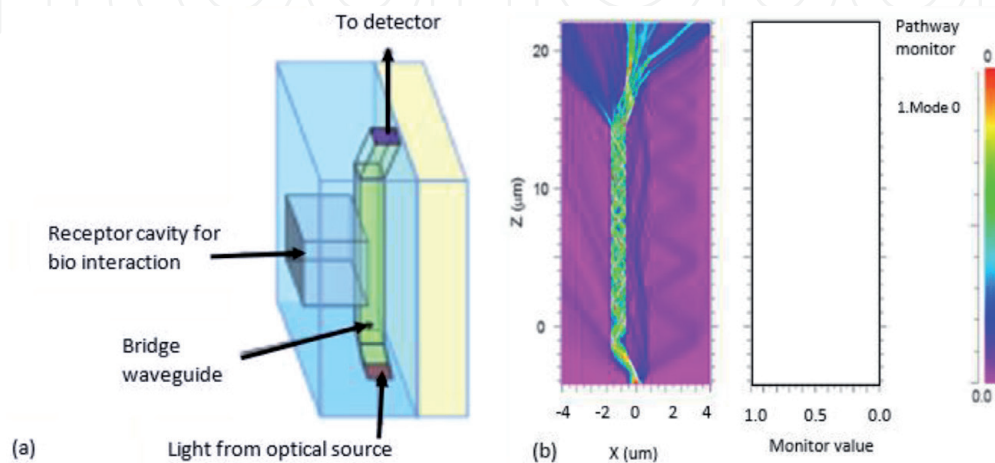


Figure 11. Bridge waveguide design realization with RSoft BeamProp optical simulation software: (a) design of bridge waveguide device [43], (b) optical simulation run for the bridge waveguide.

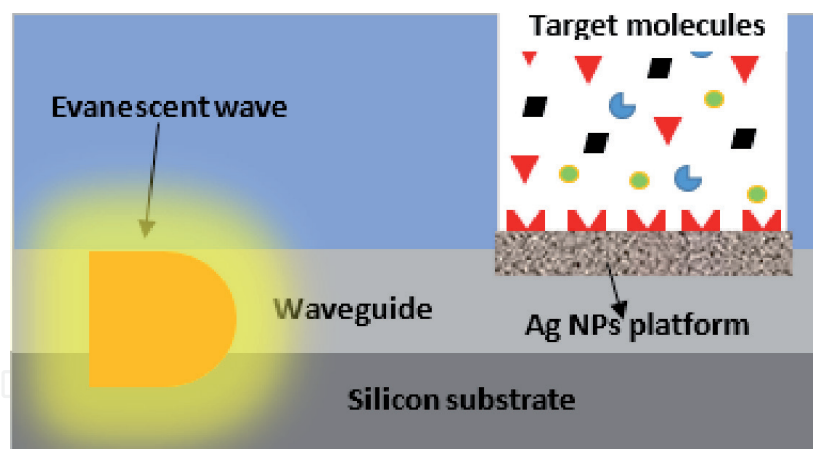


Figure 12. Application of optical biosensor based on evanescent wave interaction and nanomaterial enhancement for increased sensitivity and selectivity of target analytes in the within the cavity in the interaction area.

use of waveguide optics and intermediate evanescent-based waveguide receptor layers. An attractive feature of these applications is the micro-positioning of the optical source itself through micro- and nano-lithographic technology, the design of waveguides and wavelength dispersers using the same technology, and the design of micro-electronic processing technology in close proximity to the optical source and detectors to process and transfer derived information to adjacent on-chip processing circuitry. **Figure 12** demonstrates a typical application where the AgNPs synthesized are deployed in the etched cavity within the nitrite layer to form a highly sensitive platform for selective detection of analytes like prostate specific antigen, which is a biomarker for prostate cancer cells.

7. Conclusions

The current designs and simulations as demonstrated in this chapter indicate that it would be possible to develop simple to advanced micro and even nano sensors directly on silicon chip, by means of Si AMLEDs and standard silicon integrated circuitry processing. The design of various on-chip nano- and micro-dimensioned sensors that can detect a variety of parameters using waveguide optics and intermediate evanescent- and waveguide-based receptor layers seems possible. The major advantage of such biosensors would be the micro-dimensioning and the integration of such sensors directly on the chip, in conjunction with adjacent on-chip optical processing circuitry. Sensitivity and selectivity of such biosensor devices can be enhanced by creating a layer of nanomaterials in the receptor cavity. Since monolayers of analytes can be detected through the diversion of waveguide traveling radiation into absorbed species with different refractive indices, or through the coupling of species with the evanescent electrical fields of waveguides, the sensors could be made extremely sensitive.

Acknowledgements

This work was supported in part by the National Research Foundation's Rated Researcher Incentive Funding (IFR2011033100025 Grant), Key International Collaboration Grant (KIC 69798), and the Department of Higher Education and Training (DHET) Grant, administered by the Tshwane University of Technology, South Africa. The iNanoWS Laboratory at UNISA, South Africa, is specially

thanked for supporting the experimental analyses and facilitating the nanomaterials analysis and characterization work as presented in this chapter.

Conflict of interest

“The authors declare no conflict of interest.” or delete this entire section.

IntechOpen

Author details

Timothy Anton Okhai^{1,3*}, Azeez O. Idris², Usisipho Feleni² and Lukas W. Snyman^{2,3}

1 Clinical Engineering Cluster Group, Department of Electrical Engineering, Tshwane University of Technology, Pretoria, South Africa

2 Institute for Nanotechnology and Water Sustainability (iNanoWS), College of Science, Engineering and Technology, University of South Africa, Florida, South Africa

3 Department of Electrical Engineering, College of Science, Engineering and Technology, University of South Africa, Florida, South Africa

*Address all correspondence to: timokhai@yahoo.co.uk

IntechOpen

© 2020 The Author(s). Licensee IntechOpen. This chapter is distributed under the terms of the Creative Commons Attribution License (<http://creativecommons.org/licenses/by/3.0>), which permits unrestricted use, distribution, and reproduction in any medium, provided the original work is properly cited. 

References

- [1] Fitzgerald EA, and Kimerling LC. Silicon-based micro-photonics 627 and integrated optoelectronics. *MRS Bull*: 1998. vol. 23, no. 4, pp. 39-47.
- [2] Wada K. Electronics and photonics convergence on Si CMOS platform. In: *Proceedings of SPIE*. 2004; 5357, p. 16-24.
- [3] Alfano RR. The ultimate white light. *Sci. Amer.* 2006;295: 86-93.
- [4] Soref R. The Past, Present, and Future of Silicon Photonics. *Selected Topics in Quantum Electronics. IEEE Journal of.* 2006;12:1678-1687.
- [5] Soref R. Silicon photonics technology: past, present and future. In: Kubby JA, and Jabbour GE. Editors. *Optoelectronic Integration on Silicon II. Proceedings of SPIE*; 2008.p.5730.
- [6] Snyman LW, Ogudo KD, and Foty D. Development of a 0.75 micron wavelength CMOS optical communication system. In: *Proceedings of SPIE*; 2011; 7943.p. 79430K-1–79430K-12.
- [7] Snyman LW. Integrating Micro-Photonic Systems and MOEMS into Standard Silicon CMOS Integrated Circuitry. In: Predeep P, editor. *Optoelectronics – Devices and Applications*. Croatia; IntechOpen; 2011. p. 23-50. DOI: 10.5772/18810/978-953-51-4921-7.ch2
- [8] Xu K, Snyman LW, Polleux J-L, Chen H, and Li G. Silicon Light-Emitting Device with Application in the Micro-opto-electro-mechanical Systems. *International Journal of Materials, Mechanics and Manufacturing*. 2015; 3; 4; pp282-286. ISSN: 1793-8198
- [9] Xu K, Ogudo KA, Polleux J-L, Viana C, Ma Z, Li Z, Yu Q, Li G, and Snyman LW. Light-emitting Devices in Si CMOS and RF Bipolar Integrated Circuits. 2016; 2; 1550-2716. DOI: 10.1080/15502724.2015.1134333
- [10] Newman R. Visible light from a silicon p-n junction. *Phys. Rev.* 1955; 100; 2. 700-704.
- [11] Ghynoweth WG, and McKay KG. Photon emission from avalanche breakdown in silicon. *Physical Rev.* 1956; 102;369-376.
- [12] Dutta S, Steeneken PG, Agarwal V, Schmitz J, Annema A-J, Hueting RJE. The Avalanche-Mode Superjunction LED. *IEEE Transactions on Electron Devices*. 2017; 64; 1612-1618.
- [13] Okhai TA, Snyman LW, Polleux J-L. Wavelength dispersion characteristics of integrated Silicon Avalanche LEDs – Potential applications in futuristic on-chip micro-and nano-bio-sensors. In: *Proceedings of the SPIE Fourth Conference on Sensors, MEMS and Electro-Optic Systems (SMEOS '17)*, September 2016; Skukuza, South Africa; SPIE 2017. 10036. p. 1003604-1003604-22.
- [14] Hassibi AA, Plummer ID, and Griffin PB. Design requirements for integrated biosensor arrays. *Progress in Biomedical Optics and Imaging*. In: *Proceedings of SPIE*; 2017. 5699; 57. p. 403-413. DOI: 10.1117/12.591300
- [15] Kramer J, Seitz P, Steigmeier EF, Auderset H, and Delley B. Light-emitting devices in Industrial CMOS technology. *Sensors and Actuators*. 1993. A37-38. p 527-533.
- [16] Bude J, Sano N, and Yoshii A. Hot carrier luminescence in silicon. *Phys. Rev. B*. 1992; 45: 11. p. 5848-5856.
- [17] Akil N, Houstma VE, LeMintz P, Holleman J, Zieren V,

- DeMooij D, Woerlee PH, van den Berg A, and Wallinga H. Modelling of light-emission spectra measured on silicon nanometer-scale diode antifuses. *Journal of Applied Physics*. 2000; 88; 4. p. 1916-1922.
- [18] Moll JL and Van Overstraeten R. Charge multiplication in silicon p-n junctions. *Solid-State Electron*. 1963; 6; 2. p. 147-157.
- [19] Snyman LW, du Plessis M, Seevinck E, and Aharoni H. An efficient, low voltage, high frequency silicon CMOS light emitting device and electro-optical interface. *IEEE Electron Device Letters*. 1999; 20;12. p. 614-617.
- [20] Agah A, Hassibi I, Plummer D, and Griffin PB. Design requirements for integrated biosensor arrays. *Progress in Biomedical Optics and Imaging*. In: *Proceedings of SPIE*. 2005; 5699: 57. p. 403-413. DOI: 10.1117/12.591300
- [21] Lechuga LM. Optical biosensors. In: Gorton L. *Biosensors and Modern Biospecific Analytical Techniques*. vol. 44 of *Comprehensive Analytical Chemistry Series*. Editor. Amsterdam: Elsevier Science BV; 2005; 44. p. 209-250.
- [22] Healthcare in the palm of your hand. [Internet]. 2019. Available from: <http://qualcommtricorderxprize.org>. [Accessed: 28/12/2019].
- [23] Snyman LW, Aharoni H, du Plessis M, Marais JFK, Van Niekerk D, and Biber A. Planar light emitting electro-optical interfaces in standard silicon complementary metal oxide semiconductor integrated circuitry. *Opt. Eng.* 2002; 41. p. 3230-3240.
- [24] Booth N. and Smith AS. *Infrared Detectors*. New York and Boston. Goodwin House Publishers. 1997; p. 241-248.
- [25] Davis AR, Bush C, Harvey JC and Foley MF. Fresnel lenses in rear projection displays. In: *SID Int. Symp. Digest Tech.* 2001; 32. p. 934-937.
- [26] Van Derlofske JF. Computer modeling of LED light pipe systems for uniform display illumination. In: *Proceedings of SPIE*. 2001; 4445: p. 119-129.
- [27] Snyman LW, Xu K, Polleux J-L, Ogudo KA. and Viana C. Higher Intensity SiAvLEDs in an RF Bipolar Process Through Carrier Energy and Carrier Momentum Engineering. *IEEE Journal of Quantum Electronics*. 2015; 51; 7. P. 3200110-3200125. DOI: 10.1109/JQE.2015.2427036. (ISSN: 0018-9197).
- [28] Snyman LW, Polleux J-L, Ogudo KA, and Du Plessis M. Stimulating 600 – 650nm Wavelength Optical Emission in Monolithically Integrated Silicon LEDs through controlled Injection-Avalanche and Carrier Density Balancing Technology. *IEEE Journal of Quantum Electronics*. 2017; 53: 5. P. 1-9. DOI: 10.1109/JQE.2017.2736254 (ISSN 0018-9197).
- [29] Hassibi A, Lee TH. A programmable Electrochemical Biosensor Array in 0.18 μm . In: *International Solid State Conference*. 2005. Session 30, Displays and Biosensors,30.7
- [30] Wong HS, and White MH. A CMOS integrated ISFET-operational Amplifier Chemical Sensor Employing Differential Sensing. *IEEE Trans. on Electron devices*. 1989; 36. P. 479-498.
- [31] Schienle M, et al,. A fully Electronic DNA sensor with 128 positions and In-Pixel A/D Conversion. *ISSCC Dig. Tech. Papers*. 2004; p. 220-221.
- [32] Savran CA, Burg TP, Fritz J, and Manalis SR. Microfabricated mechanical biosensor with inherently differential readout. *Appl. Phys. Lett.* 2003; 83: 8. p. 1659.
- [33] Voiculescu I, Zaghloul ME, McGill RA, Houser EJ, and Fedder GK.

Electrostatically actuated resonant microcantilever beam in CMOS technology for the detection of chemical weapons. *IEEE Sensors J.* 2005; 5: 4. p. 641-647.

[34] Ramanathan K, and Danielsson B. Principles and applications of thermal biosensors. *Biosens. Bioelectron.* 2001; 16: 6. p. 417-423.

[35] Lechuga LM. Optical biosensors. In: Gorton L, editor. *Biosensors and Modern Biospecific Analytical Techniques*. Vol 44 of *Comprehensive Analytical Chemistry Series*. Amsterdam: Elsevier Science BV; 2005; p. 209-250.

[36] Zinoviev K, Carascosa LG, Rio JSD, Sepulveda B, Dominguez C. and Lechuga LM. Silicon photonic biosensors for lab-on-a-chip applications. *Advances in Optical Technologies.* 2008; 383927. DOI: 10.1155/2008/383927.

[37] Ogudo KA, Snyman LW, Polleux J-L, Viana C, Tegegne Z, and Schmieder D. Towards 10-40 GHz on-chip micro-optical links with all integrated Si Av LED optical sources, Si N based waveguides and Si-Ge detector technology. In: *Proceedings of SPIE.* 2014; 8991. p. 899108.

[38] Muzamil M, Khalid N, Aziz MD and Abbas SA. Synthesis of silver nanoparticles by silver salt reduction and its characterization. *Materials Science and Engineering.* 2014; 60. P. 012034. DOI: 10.1088/1757-899X/60/1/012034

[39] Devara J, Kumari P, Aarti C, and Renganathan A. Synthesis and characterization of Silver nanoparticles using cannon ball leaves and their cytotoxic activity against MCF-7 line. *Nanocomposites.* 2013; 598328. DOI: 10.1155/2013/598328

[40] Mahadevan S, Vijayakumar S, Arulmozhi P. Green synthesis of

silver nano particles from *Atalantia monophylla* (L) Correa leaf extract, their antimicrobial activity and sensing capability of H₂O₂. *Microbial Pathogenesis.* 2017; 113. p. 445-450. DOI: 10.1016/j.micpath.2017.11.029

[41] Salari S, Esmailzadeh Bahabadi S, Samzadeh-Kermani A, Yosefzadei F. In-vitro Evaluation of Antioxidant and Antibacterial Potential of GreenSynthesized Silver Nanoparticles Using *Prosopis farcta* Fruit Extract. *Iranian Journal of Pharm. Res.* 2019; 18: 1. p. 430-455. [Internet]. Available from: <https://www.ncbi.nlm.nih.gov/pmc/articles/PMC6487442/>

[42] Nilavukkarasi M, Vijayakumar S, Prathip Kumar S. Biological synthesis and characterization of silver nanoparticles with *Capparis zeylanica* L. leaf extract for potent antimicrobial and anti proliferation efficiency. *Materials Science for Energy Technologies.* 2020; 3. p. 371-376. DOI: 10.1016/j.mset.2020.02.008

[43] Xu K, Chen Y, Okhai TA, and Snyman LW. Micro optical sensors based on avalanching silicon light-emitting devices monolithically integrated on chips. *Optical Materials Express.* 2019; 9. p. 3985-3997.

[44] Venter PJ, Du Plessis M, Bogalecki AW, Goosen ME and Rademeyer P. An 8 × 64 pixel dot matrix microdisplay in 0.35 micron CMOS technology. *Optical Engineering.* 2012; 51: 014003. Du Plessis et al.: Spectral Characteristics of hot electron electroluminescence. 577

[45] Chen AR, Akinwande AI, and Lee H-S. CMOS-based microdisplay with calibrated backplane. *IEEE J. Solid-State Circuits.* 2005. P. 40:2746-2755.

[46] Rebohle L, Gebel T, Yankov RA, Trautmann T, Skorupa W, Sun J, Gauglitz G, and Frank R. Microarrays of silicon-based light emitters for

novel biosensor and lab-on-a-chip applications. *Opt. Mater.* 2005; 27. P. 1055-1058.

[47] Misiakos K, Petrou PS, Kakabakos SE, Vlahopoulou ME, Tserepi A, Gogolides E, and Ruf HH. Monolithic silicon optoelectronic transducers and elastomeric fluidic modules for bio-spotting and bio-assay experiments. *Microelectron. Eng.* 2006; 83: p. 1605-1608.

IntechOpen